Asian Journal of Current Research in Clinical Cancer
ISSN: 3062-4444
2025, Volume 5, Issue 1, Page No: 68-80

Available online at: www.galaxypub.co/page/journals

Galaxy Publication

Galaxy Publication

PLK1 Inhibitors Exhibit Potent Preclinical Activity in Platinum-Sensitive and Resistant Small Cell Lung Cancer Models

D. Toktogonov[1*], A. Isayeva[1], R. Kadyrov[1]

[1]Department of Molecular Oncology, Faculty of Medicine, University of Bishkek, Bishkek, Kyrgyzstan.

***E-mail** ✉ bishkek.molecon.97@protonmail.com

Received: 18 November 2024; **Revised:** 05 February 2025; **Accepted:** 19 February 2025

ABSTRACT

This study aimed to evaluate the preclinical activity and explore potential predictive biomarkers associated with polo-like kinase 1 (PLK1) inhibitors in experimental models of small cell lung cancer (SCLC). Cytotoxic responses to three PLK1-selective inhibitors—rigosertib, volasertib, and onvansertib—were examined across a panel of SCLC cell lines. Their therapeutic potential was further verified in subcutaneous xenografts from selected lines and in four patient-derived xenograft (PDX) systems established from both platinum-sensitive and platinum-resistant SCLC cases. Comprehensive genomic and transcriptomic analyses were conducted to determine possible markers linked to responsiveness or resistance in laboratory-developed resistant lines. All three agents—volasertib, rigosertib, and onvansertib—demonstrated potent nanomolar-level cytotoxicity against human SCLC cells in vitro. In vivo, their therapeutic effects paralleled those of standard-of-care treatments (cisplatin and irinotecan), with volasertib showing enhanced tumor growth suppression relative to cisplatin in both platinum-sensitive and resistant PDX models. Elevated YAP1 levels and loss-of-function TP53 mutations correlated with greater PLK1 inhibitor efficacy. Comparative transcriptomic profiling of onvansertib-resistant H526 derivatives revealed upregulation of NAP1L3, CYP7B1, AKAP7, and FOXG1, alongside reduced expression of RPS4Y1, KDM5D, USP9Y, and EIF1AY, indicating likely molecular resistance mechanisms. PLK1 inhibition demonstrated consistent efficacy across preclinical SCLC systems, including PDX models representing relapse under platinum sensitivity and resistance. These findings prompted the initiation of a phase II clinical investigation evaluating onvansertib in SCLC patients (ClinicalTrials.gov identifier: NCT05450965).

Keywords: Small cell lung carcinoma, PLK1 blockade, Patient-derived xenografts, Volasertib, Onvansertib

How to Cite This Article: Toktogonov D, Isayeva A, Kadyrov R. PLK1 Inhibitors Exhibit Potent Preclinical Activity in Platinum-Sensitive and Resistant Small Cell Lung Cancer Models. Asian J Curr Res Clin Cancer. 2025;5(1):68-80. https://doi.org/10.51847/vbnoiDzIdm

Introduction

Small cell lung cancer (SCLC) remains a major oncologic challenge, with over 180, 000 new diagnoses globally each year [1, 2]. Although first-line chemoimmunotherapy has yielded incremental progress [3-7], disease recurrence after initial response remains nearly universal, and salvage options continue to be ineffective [8-12]. Precision oncology approaches have revolutionized treatment for molecularly defined non-small cell lung cancer (NSCLC) subgroups—such as EGFR, ALK, and ROS1 alterations—contributing substantially to reduced lung cancer mortality over the last two decades [5, 13-17]. However, translation of such strategies into SCLC care has lagged, largely due to the predominance of tumor suppressor gene inactivation (TP53, RB1), which currently lacks viable pharmacologic targets [18-21]. Thus, novel molecularly informed interventions are urgently required.

The polo-like kinase (PLK) family of serine/threonine kinases—comprising PLK1-PLK5—regulates key checkpoints in mitotic progression and cellular proliferation [22-26]. Aberrant activation of PLKs, particularly PLK1, has been strongly linked to tumorigenesis, including in pulmonary malignancies [22, 23, 27, 28]. Given its central role, PLK1 has become a major pharmacological target in anticancer research [29].

Following initial low-throughput drug screening, PLK1 inhibitors emerged as promising therapeutic candidates for SCLC. We validated the antitumor impact of onvansertib, a clinically relevant PLK1 blocker, in patient-

derived xenograft (PDX) systems. Sensitivity was most pronounced within YAP1-enriched subtypes and in tumors harboring disruptive p53 mutations, irrespective of subtype. These biomarkers guided the design of a currently active phase II clinical trial (NCT05450965) evaluating onvansertib efficacy in SCLC.

Materials and Methods

Reagents

Volasertib, rigosertib, and onvansertib were sourced from Selleckchem (Houston, TX, USA). Stock compounds were solubilized in DMSO, portioned, and kept at −20 °C for in vitro work or freshly reconstituted in PBS for xenograft use. Clinical-grade cisplatin (Teva Parenteral Medicines, Irvine, CA, USA) and irinotecan were obtained from institutional hospital pharmacies. Primary antibodies used for immunoblotting included GAPDH (#sc-47724), TP53 (#sc-126) (Santa Cruz Biotechnology, Dallas, TX, USA); POU2F3 (#36135), ASCL1 (#10585), NEUROD1 (#7019), YAP1 (#14074), PLK1 (#4513), and CMYC (#5605) (Cell Signaling Technology, Danvers, MA, USA).

Cell lines and PDX models

Nine human SCLC lines (H146, H187, H128, H69, H209, DMS153, H526, DMS114, DMS53) were procured from the American Type Culture Collection (ATCC, Manassas, VA, USA). Authentication via STR profiling and mycoplasma screening was completed prior to experimentation. Cells were maintained under previously detailed culture conditions [30], generally in RPMI-1640 or Waymouth medium (for DMS lines) supplemented with 5-10% FBS, incubated at 37 °C, 5% CO_2, and 95% humidity. Four PDX models (TKO-002, TKO-005, TKO-008, TKO-010) from our institutional tumor repository [31] were used for in vivo studies, with TKO-002, TKO-005, and TKO-010 classified as ASCL1, and TKO-008 as NEUROD1 subtype.

In vitro cytotoxicity assay

SCLC cells were seeded into 96-well plates (0.5-3 × 10^4 cells/well). After 24 h, cells were continuously treated with vehicle or target compounds for 72 h. Cell proliferation was quantified using MTS (Promega) or WST-1 (Takara Bio USA) assays, following manufacturer guidelines. For densely aggregating lines (H526, H209, H187), the CellTiter-Glo 3D viability kit (Promega) was applied. Absorbance/luminescence was read on a Tecan Infinite M1000 Pro reader (Switzerland). Half-maximal inhibitory concentrations (IC_{50}) were determined via GraphPad Prism v9 (GraphPad Software, La Jolla, CA, USA).

Western blotting

Whole-cell lysate preparation and immunoblot procedures followed established protocols [30, 32].

In vivo tumor growth assessment

All experiments involving animals were carried out in compliance with approved protocols from the Institutional Animal Care and Use Committee to ensure humane treatment. Xenograft tumors were established in 6-week-old athymic (nu/nu) mice obtained from Harlan Industries (Indianapolis, IN, USA). Mice were maintained under pathogen-free conditions in microisolator cages and provided unrestricted access to standard chow and water. H526 cells (1-2 × 10^7) suspended in serum-free medium were combined with Matrigel and injected subcutaneously into the flank of each mouse. Patient-derived xenograft (PDX) experiments followed previously published protocols [31]. Tumor growth was monitored until volumes reached roughly 100 mm^3. Mice with comparable tumor sizes and body weights were randomly assigned to treatment groups of six to eight animals. Treatment regimens included volasertib (20 mg/kg, intraperitoneally, weekly), cisplatin (3 mg/kg, weekly IP), irinotecan (25 mg/kg, weekly IP), rigosertib (250 mg/kg, daily IP), and onvansertib (60 mg/kg, orally, daily for 10 days with a 4-day drug-free interval). Tumor dimensions ($V = ½ \times \text{length} \times \text{width}^2$) and body weights were recorded twice per week. At the end of the study, tumors were excised and weighed.

Whole-transcriptome and pathway analyses

We retrieved previously generated gene expression datasets of human SCLC cell lines from the Illumina HT-12 platform, deposited in NCBI GEO (GSE55830) [30]. Raw intensities from untreated cells were normalized using quantile normalization in GenomeStudio (v2.0, Illumina) and then $\log_2$-transformed for downstream analyses.

Supervised clustering was performed based on MYC, PLK1, and TP53 expression levels. IC_{50} values of PLK1 inhibitors were compared between these clusters.
Differential expression analysis was also performed using DepMap 21Q1 SCLC datasets [33], comprising 48 cell lines (9 SCLC-Y subtype, 39 other subtypes). $Log_2(x + 1)$-transformed RNA-seq TPM values were extracted from CCLE_expression.csv. Fold changes were computed by comparing the mean gene expression of SCLC-Y versus non-SCLC-Y groups. Drug sensitivity data were obtained from the GDSC portal [34]. Statistical significance was evaluated using t-tests, and q-values were calculated with the Benjamini-Hochberg correction.

Generation of onvansertib-resistant H526 cells
H526 cells resistant to onvansertib were established by continuous culture with gradually increasing concentrations of the drug (10-75 nM) over one year. RNA was extracted from both parental and resistant cells in triplicate using the Qiagen RNeasy kit. RNA-seq was conducted by Novogene (Durham, NC, USA). Reads were preprocessed to remove adapters and low-quality bases using Trimmomatic v0.38. RSEM v1.3.1 was used to align reads to the GRCh38 reference genome, and gene counts were quantified using Gencode v43 annotations. Differential expression analysis was performed with DESeq2, fitting a negative binomial generalized linear model for each gene. The Wald test was applied to assess statistical significance, reporting log fold changes, p-values, and adjusted p-values. Sequencing data were submitted to GEO (GSE269636).

Statistical analysis
Differences in IC_{50} values across PLK1 inhibitors were assessed using ANOVA or the Kruskal-Wallis test, as appropriate. Correlations between drug sensitivity and cell line response were calculated using Pearson or Spearman coefficients. Tumor growth inhibition relative to control was determined using %T/C = [(mean tumor volume in treated group on day X ÷ mean tumor volume in control group on day X) × 100]. Mixed-effects models were used to analyze overall and pairwise differences in tumor volume among treatments. Differences in tumor weights at study end were evaluated using ANOVA. All analyses were conducted in SAS 9.3 and GraphPad, with $p < 0.05$ considered significant. Differential gene expression and drug sensitivity analyses were carried out using Python.

Results and Discussion

Low-throughput screening of targeted compounds in SCLC
To discover potential therapeutic candidates for SCLC, a low-throughput, non-biased screen was used to assess the in vitro cytotoxicity of compounds not previously investigated in SCLC clinical trials. Nanomolar activity was predefined as the minimum threshold for advancing a compound to detailed preclinical evaluation. Ten agents were tested in a panel of SCLC lines (H526, H187, H69, H209, H146, DMS153, DMS114, DMS53) with well-characterized genomic and transcriptomic profiles **(Figure 1d)**.
The compounds targeted HSP90 (AUY922), CHK1 (MK8776), CDK (SCH727965), MEK (MEK162), CHK1/2 (AZD7762), PIK3CA (BKM120), WEE1 (MK1775), PLK1 (rigosertib, volasertib), and BRD (JQ-1). Agents against PLK1, CDK, and HSP90 met the pre-set cytotoxicity threshold **(Figure 1a)**. Some compounds were deprioritized due to safety concerns (SCH727965) or discontinued industrial support (AUY922). PLK1 inhibitors demonstrated the strongest nanomolar activity across SCLC lines (rigosertib and volasertib, BI6727) **(Figures 1a and 1b)**. Considering PLK1's central role in regulating RB1 and P53-mediated cell cycle effects, further studies focused on this class. Onvansertib, a highly specific PLK1 inhibitor, was then tested on the same panel, confirming the high sensitivity of SCLC cells **(Figure 1c)**.

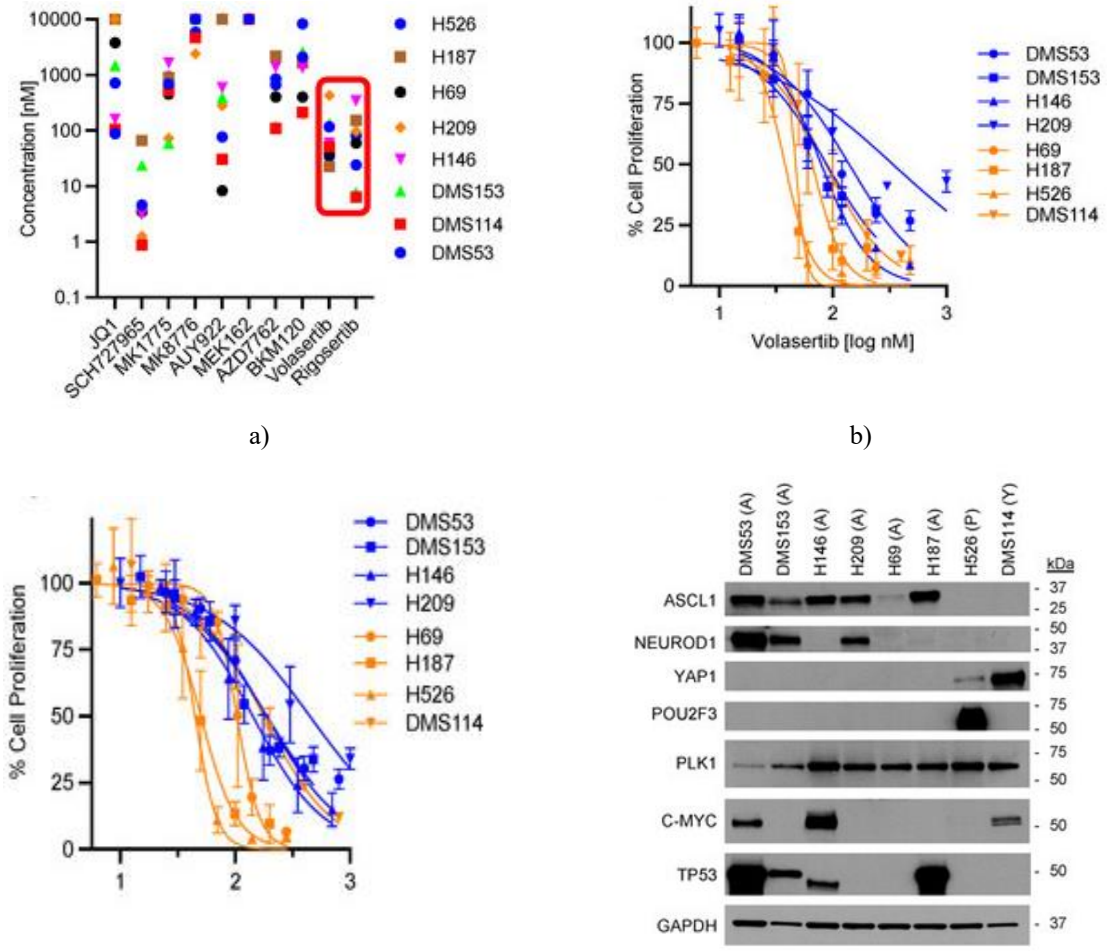

Figure 1. Evaluation of the antiproliferative response of precision agents in small-cell lung cancer (SCLC) lines. (a) Screening of multiple SCLC cell lines; (b) and (c) illustrate the actions of volasertib and onvansertib on cellular proliferation. Treatments were administered for 72 hours with the compounds shown. Cell growth was quantified using either luminescent or colorimetric detection, depending on cell aggregation behavior in culture. Results are expressed as mean ± S.D., based on no fewer than three independent replicates. Blue and orange plots correspond to p53 non-disruptive and disruptive mutations, respectively. (d) displays basal protein levels in SCLC cell lines, where molecular subtypes are indicated by ASCL1 (A), POU2F3 (P), or YAP1 (Y).

In vivo validation of PLK1 inhibition

To determine if in vitro responses translated to in vivo antitumor benefit, and to compare PLK1 blockade with conventional chemotherapy in SCLC, we performed xenograft studies. Mice with tumors derived from the H526 line—the most responsive line from initial screening—received weekly intraperitoneal (i.p.) doses of volasertib (20 mg/kg), cisplatin (3 mg/kg), or irinotecan (25 mg/kg). In this model, volasertib induced marked tumor reduction relative to vehicle control but displayed slightly lower efficacy than irinotecan or cisplatin **(Figure 2)**. Body weights showed no significant difference between treated and untreated groups, indicating acceptable tolerability.

Patient-derived xenografts (PDXs) are known to more accurately mimic therapeutic behavior in humans compared to subcutaneous models [35, 36]. Earlier research confirmed that rigosertib, a prototype PLK1 blocker, exhibited tumor inhibition comparable to cisplatin in an SCLC PDX study [31]. Building on this, we analyzed PLK1 inhibition across four PDX models. Beyond first-generation inhibitors, onvansertib (NMS-P937; PCM-075; NMS1286937) was tested—a selective oral agent with over 5000-fold affinity for PLK1 relative to PLK2/PLK3, now under clinical assessment [37]. Onvansertib has shown promising single-agent and combination results in hematologic, colorectal, and prostate malignancies [37-39]. Consistent with volasertib and rigosertib findings, onvansertib demonstrated potent nanomolar activity in vitro against SCLC cell lines **(Figure 1c)**. Furthermore, it

significantly suppressed tumor expansion in both platinum-resistant (TKO-002, TKO-008; **(Figures 3a and 3b))** and platinum-sensitive (TKO-005, TKO-010; **(Figures 3c and 3d))** PDXs, outperforming cisplatin. No substantial loss in body weight or treatment-related toxicity was observed in any group.

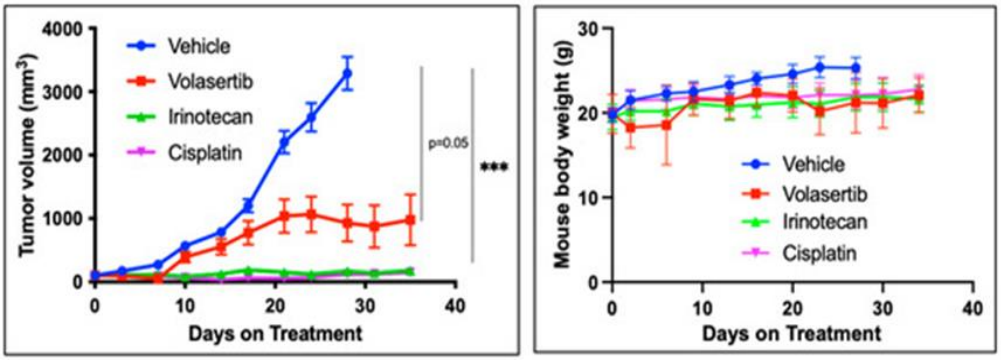

Figure 2. In vivo antitumor performance of PLK1-targeted therapy in SCLC. Mice bearing H526 tumors were treated weekly by i.p. injection with volasertib (20 mg/kg), irinotecan (25 mg/kg), or cisplatin (3 mg/kg). Data represent mean ± SEM for six subjects per cohort. *** $p \leq 0.001$.

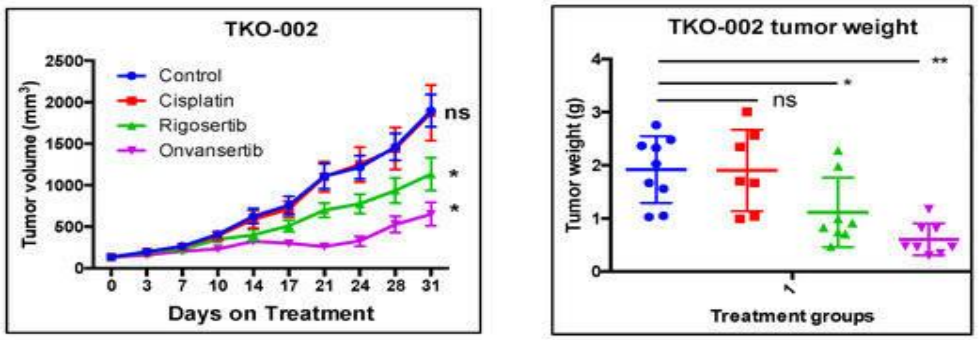

a)

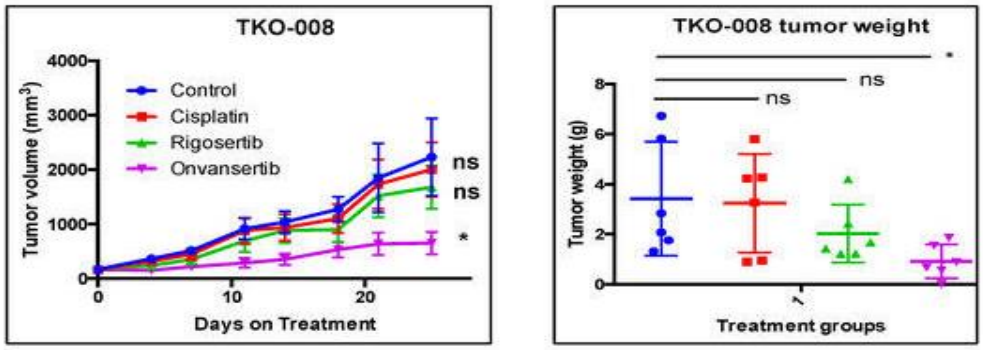

b)

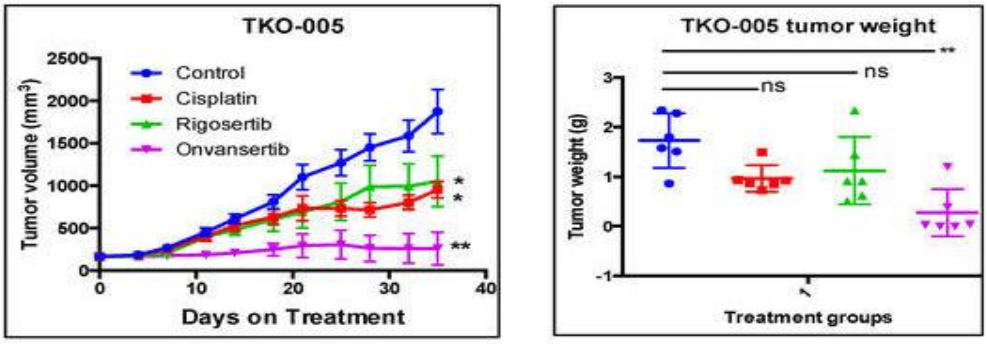

c)

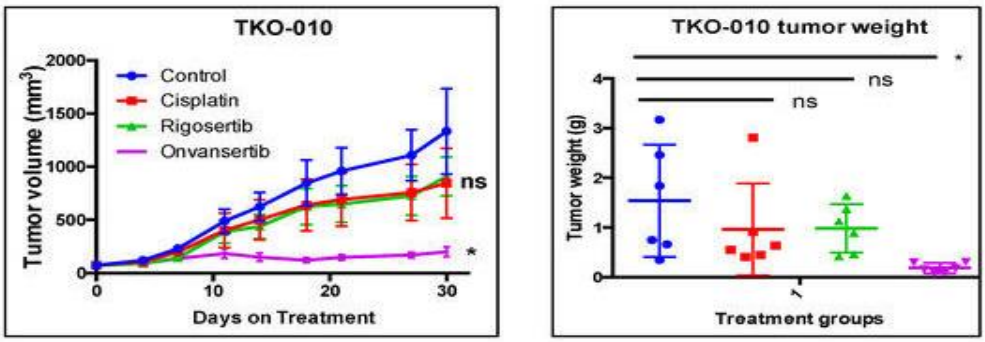

d)

Figure 3. Anticancer potential of PLK1 blockade in SCLC PDXs. Platinum-resistant models (TKO-002, TKO-008; a, b) and platinum-sensitive models (TKO-005, TKO-010; c, d) were administered cisplatin (3 mg/kg; i.p. weekly), rigosertib (250 mg/kg; i.p. daily), and onvansertib (60 mg/kg; orally for 10 consecutive days, followed by 4 rest days). Tumor volumes are shown as mean ± S.D. from six mice per group. * indicates significant; ns = not significant versus control. * $p \leq 0.05$, ** $p \leq 0.01$.

Transcriptomic correlates of PLK1 inhibitor sensitivity in SCLC

Despite their nanomolar in vitro potency, PLK1 inhibitors exhibited variable IC_{50} ranges among SCLC cell lines **(Figures 1b and 1c; Table 1)**. Using the overall median IC_{50} as a divider, the highly responsive group showed a mean IC_{50} for volasertib of 40 nM, roughly ten times lower than the less responsive group's 550 nM **(Table 1)**. Similar differences were noted for onvansertib and rigosertib.

To explore if genetic or transcriptional factors could forecast drug sensitivity, gene expression data from the NCBI GEO dataset GSE55830 [30] were analyzed. Normalized levels of TP53, PLK1, and MYC were compared between high- and low-sensitivity groups. No significant expression changes were detected **(Figure 4a)**. Further exploration via the SclcCellMinerCDB database (68 SCLC lines) also revealed no direct association between PLK1 mRNA levels and volasertib response. Elevated MYC expression correlated with increased sensitivity trends, and TP53 expression was significantly higher in the lines most responsive to volasertib treatment.

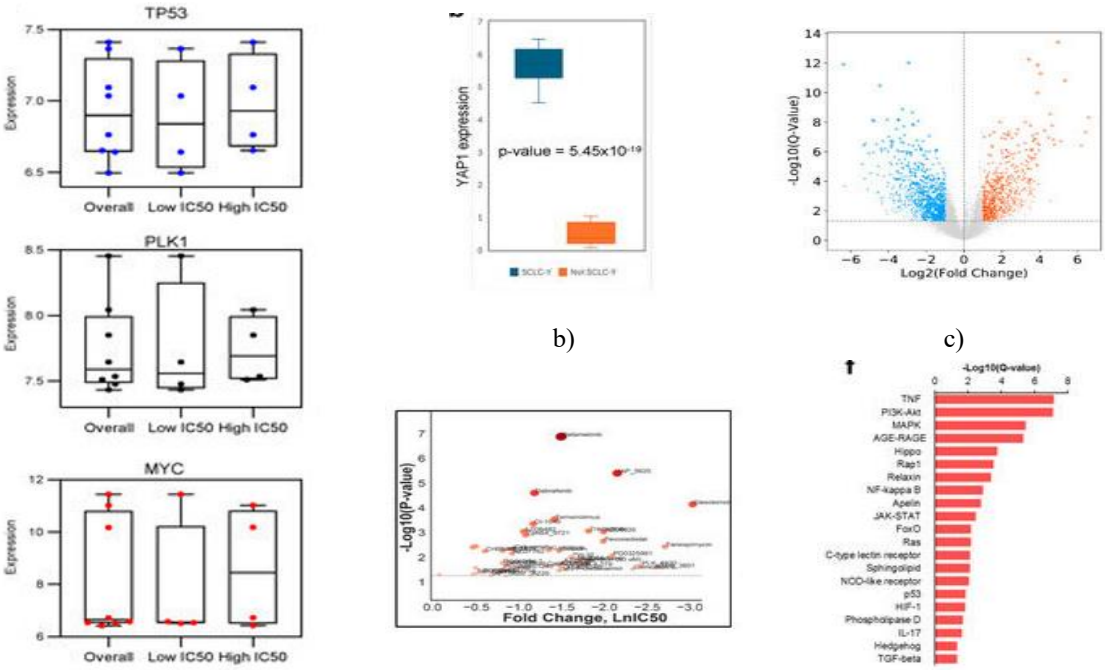

a) b) c) d) **f)**

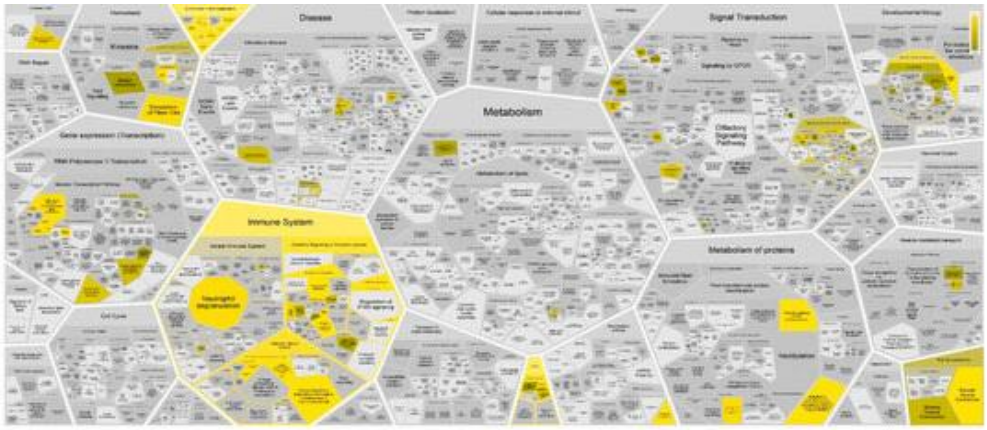

e)

Figure 4. Comparative transcriptomic analyses: expression correlation between TP53, PLK1, and MYC (NCBI GEO GSE55830 [30]) and PLK1 inhibitor sensitivity (a); YAP1 expression in SCLC-Y versus other subtypes (b); volcano plot displaying genes differentially expressed between SCLC-Y and non-SCLC-Y lines (c); evaluation of therapeutic vulnerability suggesting PLK1 inhibition as a promising target in YAP1-positive lines (d); Reactome-based functional mapping revealing immune and muscle-related pathway variations (e); KEGG signaling enrichment showing differential pathway activation between both categories (f).

Table 1. IC_{50}-based drug sensitivity of SCLC cell lines to PLK1 inhibitors.

Cell Line	Volasertib (nM)	Onvansertib (nM)	Rigosertib (nM)	TP53 Gene Mutation	Hemizygous Deletion
DMS53	139.9 ± 21.8	188.9 ± 36.2	153.6 ± 23.7	c.722C > T	No
DMS153	90.0 ± 15.9	181.2 ± 36.8	114.8 ± 22.9	c.463A > C	No
H146	78.1 ± 14.5	145.3 ± 62.0	93.2 ± 16.9	Wild type	No
H209	550.7 ± 170.1	710.4 ± 260.0	385.7 ± 130.9	c.673-2A > T	No
H69 *	64.1 ± 19.9	105.1 ± 12.4	71.9 ± 19.0	c.511G > T	Yes
H187 *	40.4 ± 8.9	55.7 ± 19.3	61.8 ± 24.7	c.722C > G	Yes
H526 *	49.6 ± 14.3	51.4 ± 15.2	123.9 ± 32.6	c.97-1G > C	Yes
DMS114 *	87.1 ± 21.3	196.7 ± 58.6	52.3 ± 10.3	c.637C > T	Yes

Denotes concurrent hemizygous loss. Cytotoxicity profiles were established across a representative SCLC panel covering multiple transcriptomic classes. Mean IC_{50} values reflect the average of three to five separate experiments.

The recently characterized molecular subtypes of small-cell lung cancer (SCLC) are primarily classified by dominant expression of specific transcriptional regulators: achaete-scute homolog 1 (ASCL1), neurogenic differentiation factor 1 (NEUROD1), POU domain class 2 transcription factor 3 (POU2F3), and the transcriptional coactivator YAP1 [40-42]. Each subtype demonstrates distinctive gene expression signatures. For example, the non-neuroendocrine SCLC variants display higher levels of MYC expression, and in murine models, MYC activation has been shown to promote a phenotypic switch from neuroendocrine SCLC-A and SCLC-N to the non-neuroendocrine SCLC-Y type [43, 44].

Accordingly, we utilized publicly accessible datasets from the Genomics of Drug Sensitivity in Cancer (GDSC; https://www.cancerrxgene.org/, accessed 7 May 2021) and the Cancer Dependency Map (https://depmap.org/portal/, accessed 6 May 2021) to perform an unbiased analysis comparing therapeutic susceptibility between the SCLC-Y subtype and other transcriptional classes **(Figure 4b)**. From this analysis, we identified differentially expressed genes (DEGs) that might suggest heightened drug sensitivity in YAP1-enriched cell lines **(Figure 4c)**. Further examination through the Cancer Therapeutics Response Portal revealed a number of potential compounds—most notably PLK1 inhibitors—that displayed selective and robust efficacy in SCLC-Y models **(Figure 4d)**. These findings confirmed our preliminary low-throughput screening results, highlighting PLK1 inhibitors as promising therapeutic agents.

Interestingly, gene set enrichment analysis (GSEA) performed with the Reactome database [45] showed that YAP1-positive cells exhibited elevated expression of immune-related genes **(Figure 4e)**. In parallel, KEGG pathway mapping of DEGs indicated enrichment of several signaling routes, including TNF, PI3K/AKT, MAPK, AGE-RAGE, and Hippo pathways **(Figure 4f)**.

TP53 gene alterations and response to PLK1 blockade

Previous research has associated TP53 mutations with sensitivity to PLK1 inhibition [46-51], whereas cells maintaining normal diploid karyotypes typically exhibit resistance [48, 49, 52]. Conversely, other investigations have found no significant association between TP53 mutation status and PLK1 inhibitor response [53]. We proposed that these discrepancies might stem from differences in how specific TP53 mutations affect p53 protein function.

To explore this, we correlated the cytotoxic potency (IC_{50} values) of PLK1 inhibitors with the predicted functional outcomes of TP53 mutations identified in our SCLC line panel through targeted DNA sequencing [30, 54]. As expected, TP53 mutations were highly prevalent (seven of eight lines), consistent with prior studies [18-21]. Notably, four cell lines—H526, H69, H187, and DMS114—harboring concurrent hemizygous deletions of TP53 displayed markedly greater sensitivity than those retaining wild-type alleles or lacking such deletions **(Table 1; Figure 5a)**. These findings suggest that functional inactivation of TP53 enhances susceptibility to PLK1 inhibition, consistent with existing evidence [51].

Although TP53 mutation is nearly universal in SCLC, its biological impact depends on mutation type and location. Using the Cancer Cell Line Encyclopedia via cBioPortal (https://www.cbioportal.org), we cataloged the specific variants found in SCLC cell lines and tumor tissues.

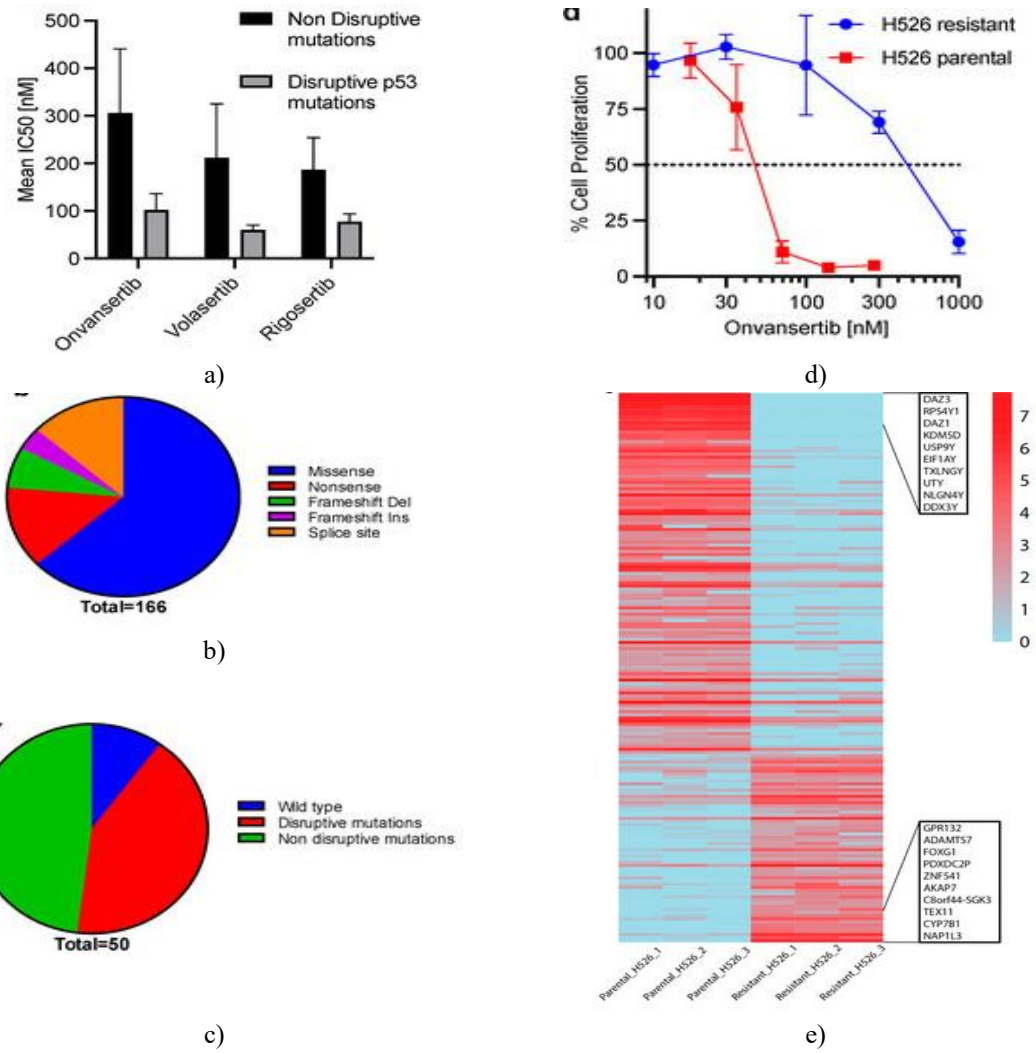

Figure 5. Effect of TP53 mutational status on PLK1 inhibitor activity. Comparison of mean IC_{50} by TP53 mutation category (a); TP53 gene profiles in 166 tumors from cBioPortal (b); TP53 mutation distribution

among 50 SCLC lines in CCLE (c); PLK1 inhibitor activity in parental versus resistant H526 cells (IC_{50}: 51 nM vs. 447 nM) (d); gene expression profiles from three biological replicates of parental and resistant H526 cells (e). The heatmap highlights the top DEGs (p-adj < 0.5; logFC > 4), with red and blue indicating elevated and reduced expression, respectively.

As expected, TP53 variants were both common and diverse in their effects **(Figure 5b)**. Roughly 60% represented non-disruptive forms, while 40% were disruptive inactivating mutations predicted to abolish p53 function **(Figure 5c)**. These observations align with previous reports showing that TP53 loss or inactivating mutations increase vulnerability to PLK1 inhibitors, whereas wild-type or gain-of-function (GOF) variants attenuate sensitivity [46-51]. Overall, our data indicate that disruptive TP53 alterations—such as hemizygous deletions or truncations—enhance PLK1 inhibitor response, while non-disruptive (in-frame, missense, or GOF) changes tend not to. We therefore propose that TP53 mutation classification (disruptive vs. non-disruptive) could serve as a predictive biomarker for PLK1-targeted therapies.

Differential gene expression and acquired PLK1 inhibitor resistance

A persistent issue with targeted cancer therapies is the eventual emergence of drug resistance. Identifying the molecular basis of this adaptation can guide strategies to extend drug effectiveness or restore sensitivity. To investigate mechanisms of resistance, we established PLK1 inhibitor-resistant SCLC cells through continuous exposure of parental H526 cells to increasing concentrations of onvansertib **(Figure 5d)**. Upon confirmation of stable resistance, transcriptomic comparisons were performed between parental and resistant lines to pinpoint key DEGs.

Resistant H526 cells displayed reduced expression of RPS4Y1, KDM5D, USP9Y, and EIF1AY, accompanied by increased expression of NAP1L3, CYP7B1, AKAP7, and FOXG1 **(Figure 5e)**.

SCLC remains a highly lethal malignancy with limited therapeutic progress. Although the past two decades have seen substantial advances in targeted therapies for non-small cell lung cancer, comparable breakthroughs have not occurred in SCLC—largely due to its complex biology and scarcity of actionable genomic drivers.

In this study, we evaluated several molecularly targeted compounds and found that PLK1 inhibitors exhibited strong in vitro cytotoxicity across SCLC cell lines. This effect was further confirmed in vivo, where three PLK1 inhibitors—rigosertib, volasertib, and onvansertib—produced significant tumor suppression. Notably, the robust response of onvansertib in both platinum-sensitive and platinum-resistant PDX models underscores its potential clinical value and supports the initiation of an ongoing clinical trial in relapsed SCLC (NCT05450965).

Our screening methodology intentionally employed a focused low-throughput strategy using clinically relevant agents to facilitate direct translation of promising results to patient settings. Although this approach limited the exploratory scope, it prioritized clinical feasibility and speed. The discovery of PLK1 inhibitors as strong candidates and the identification of YAP1 expression as a possible predictive marker are in line with independent studies by other groups [40, 55, 56].

The identification of potential biomarkers capable of predicting patient response to PLK1 inhibitors in clinical contexts represents an important step toward implementing precision medicine for SCLC. Across our panel of SCLC cell lines, no significant correlation was detected between PLK1 expression at the transcriptomic level and the observed in vitro cytotoxic effects of PLK1-targeting compounds. Notably, however, loss-of-function alterations—either alone or accompanied by hemizygous deletions—within the TP53 gene were linked to enhanced drug sensitivity. These outcomes align with earlier reports suggesting that total TP53 inactivation or deleterious mutations heighten susceptibility to PLK1 inhibition, whereas gain-of-function (GOF) or preserved wild-type TP53 activity mitigates responsiveness [46-51].

Among all human malignancies, TP53 stands as one of the most frequently altered genes, though the mutation rates vary substantially by tumor type—from under 5% in cervical cancer to roughly 80-90% in SCLC [57-59]. Functionally, p53 operates as both a transcriptional activator and repressor, regulating hundreds of genes [60]. While non-synonymous single-nucleotide variants are the predominant damaging TP53 changes, deletions and other genomic mechanisms also occur. Over 45, 000 unique TP53 mutations have been documented, encompassing roughly 1, 540 single-nucleotide substitutions and 2, 000 frameshift variants [60].

The biological impact of a mutation largely depends on its position—particularly within exons 5-8, which encode the DNA-binding region of p53. Disruptive mutations typically occur within the L2 (codons 163-195) or L3 (codons 236-251) motifs or introduce premature stop codons, whereas non-disruptive mutations occur outside

these zones. Considering that nearly all SCLC cases harbor TP53 mutations, and that TP53 loss is indispensable for SCLC formation in murine models [61], we proposed leveraging the biological distinction between inactivating and GOF TP53 variants to personalize therapy.

Moreover, gene set enrichment analysis comparing resistant and parental cell lines revealed pronounced modulation of immune-regulatory gene expression in resistant models. This observation warrants further study to evaluate whether combining PLK1 blockade with immune checkpoint inhibition could provide additional therapeutic benefits.

Conclusion

Our investigation identified PLK1 as a promising therapeutic target in preclinical SCLC systems. Two structurally distinct and highly selective PLK1 inhibitors—volasertib and onvansertib—demonstrated strong antitumor efficacy across in vitro studies, conventional xenografts, and patient-derived xenograft (PDX) models representing both platinum-sensitive and resistant SCLC. We further highlighted inactivating TP53 mutations and elevated YAP1 expression as potential biomarkers to refine patient selection in future clinical applications.

This preclinical evidence has progressed into clinical testing through an ongoing phase II trial of onvansertib in relapsed SCLC (NCT05450965). Additionally, onvansertib is under active evaluation in combination with standard chemotherapy for several malignancies, including KRAS-mutant metastatic colorectal cancer, metastatic pancreatic cancer, and triple-negative breast cancer. Early data from the randomized phase II mCRC trial (NCT05593328) demonstrate a 64% objective response rate (ORR), substantially exceeding that of chemotherapy alone (33% ORR).

Acknowledgments: None

Conflict of Interest: None

Financial Support: None

Ethics Statement: None

References

1. Siegel RL, Miller KD, Jemal A. Cancer statistics, 2016. CA Cancer J Clin. 2016;66(1):7–30.
2. Torre LA, Bray F, Siegel RL, Ferlay J, Lortet-Tieulent J, Jemal A. Global cancer statistics, 2012. CA Cancer J Clin. 2015;65(2):87–108.
3. Paz-Ares L, Dvorkin M, Chen Y, Reinmuth N, Hotta K, Trukhin D, et al. Durvalumab plus platinum-etoposide versus platinum-etoposide in first-line treatment of extensive-stage small-cell lung cancer (CASPIAN): A randomised, controlled, open-label, phase 3 trial. Lancet. 2019;394(10212):1929–39.
4. Horn L, Mansfield AS, Szczesna A, Havel L, Krzakowski M, Hochmair MJ, et al. First-line atezolizumab plus chemotherapy in extensive-stage small-cell lung cancer. N Engl J Med. 2018;379(23):2220–9.
5. Siegel RL, Miller KD, Fuchs HE, Jemal A. Cancer statistics, 2021. CA Cancer J Clin. 2021;71(1):7–33.
6. Behera M, Ragin C, Kim S, Pillai RN, Chen Z, Steuer CE, et al. Trends, predictors, and impact of systemic chemotherapy in small cell lung cancer patients between 1985 and 2005. Cancer. 2015;122(1):50–60.
7. Pillai RN, Owonikoko TK. Small cell lung cancer: Therapies and targets. Semin Oncol. 2014;41(2):133–42.
8. Schiller JH, Adak S, Cella D, DeVore RF 3rd, Johnson DH. Topotecan versus observation after cisplatin plus etoposide in extensive-stage small-cell lung cancer: E7593—A phase III trial of the Eastern Cooperative Oncology Group. J Clin Oncol. 2001;19(8):2114–22.
9. Schiller JH, Kim K, Hutson P, DeVore R, Glick J, Stewart J, et al. Phase II study of topotecan in patients with extensive-stage small-cell carcinoma of the lung: An Eastern Cooperative Oncology Group Trial. J Clin Oncol. 1996;14(8):2345–52.
10. von Pawel J, Jotte R, Spigel DR, O'Brien ME, Socinski MA, Mezger J, et al. Randomized phase III trial of amrubicin versus topotecan as second-line treatment for patients with small-cell lung cancer. J Clin Oncol. 2014;32(36):4012–9.

11. von Pawel J, Schiller JH, Shepherd FA, Fields SZ, Kleisbauer JP, Chrysson NG, et al. Topotecan versus cyclophosphamide, doxorubicin, and vincristine for the treatment of recurrent small-cell lung cancer. J Clin Oncol. 1999;17(2):658–67.
12. Evans TL, Cho BC, Udud K, Fischer JR, Shepherd FA, Martinez P, et al. Cabazitaxel versus topotecan in patients with small-cell lung cancer with progressive disease during or after first-line platinum-based chemotherapy. J Thorac Oncol. 2015;10(8):1221–8.
13. Shaw AT, Kim DW, Nakagawa K, Seto T, Crino L, Ahn MJ, et al. Crizotinib versus chemotherapy in advanced ALK-positive lung cancer. N Engl J Med. 2013;368(25):2385–95.
14. Shaw AT, Mehra R, Kim DW, Felip E, Chow LQM, Camidge DR, et al. Clinical activity of the ALK inhibitor LDK378 in advanced, ALK-positive NSCLC. J Clin Oncol. 2013;31(Suppl 15):8010.
15. Mok TS, Wu YL, Thongprasert S, Yang CH, Chu DT, Saijo N, et al. Gefitinib or carboplatin-paclitaxel in pulmonary adenocarcinoma. N Engl J Med. 2009;361(10):947–57.
16. Kris MG, Johnson BE, Berry LD, Kwiatkowski DJ, Iafrate AJ, Wistuba II, et al. Using multiplexed assays of oncogenic drivers in lung cancers to select targeted drugs. JAMA. 2014;311(19):1998–2006.
17. Howlader N, Forjaz G, Mooradian MJ, Meza R, Kong CY, Cronin KA, et al. The effect of advances in lung-cancer treatment on population mortality. N Engl J Med. 2020;383(7):640–9.
18. Rudin CM, Durinck S, Stawiski EW, Poirier JT, Modrusan Z, Shames DS, et al. Comprehensive genomic analysis identifies SOX2 as a frequently amplified gene in small-cell lung cancer. Nat Genet. 2012;44(10):1111–6.
19. Iwakawa R, Takenaka M, Kohno T, Shimada Y, Totoki Y, Shibata T, et al. Genome-wide identification of genes with amplification and/or fusion in small cell lung cancer. Genes Chromosomes Cancer. 2013;52(9):802–16.
20. George J, Lim JS, Jang SJ, Cun Y, Ozretic L, Kong G, et al. Comprehensive genomic profiles of small cell lung cancer. Nature. 2015;524(7563):47–53.
21. Peifer M, Fernandez-Cuesta L, Sos ML, George J, Seidel D, Kasper LH, et al. Integrative genome analyses identify key somatic driver mutations of small-cell lung cancer. Nat Genet. 2012;44(10):1104–10.
22. Zitouni S, Nabais C, Jana SC, Guerrero A, Bettencourt-Dias M. Polo-like kinases: Structural variations lead to multiple functions. Nat Rev Mol Cell Biol. 2014;15(7):433–52.
23. Lee KS, Park JE, Kang YH, Kim TS, Bang JK. Mechanisms underlying Plk1 polo-box domain-mediated biological processes and their physiological significance. Mol Cells. 2014;37(4):286–94.
24. Cholewa BD, Liu X, Ahmad N. The role of polo-like kinase 1 in carcinogenesis: Cause or consequence? Cancer Res. 2013;73(21):6848–55.
25. Clay FJ, McEwen SJ, Bertoncello I, Wilks AF, Dunn AR. Identification and cloning of a protein kinase-encoding mouse gene, Plk, related to the polo gene of Drosophila. Proc Natl Acad Sci U S A. 1993;90(10):4882–6.
26. Lee KS, Grenfell TZ, Yarm FR, Erikson RL. Mutation of the polo-box disrupts localization and mitotic functions of the mammalian polo kinase Plk. Proc Natl Acad Sci U S A. 1998;95(16):9301–6.
27. Strebhardt K. Multifaceted polo-like kinases: Drug targets and antitargets for cancer therapy. Nat Rev Drug Discov. 2010;9(8):643–60.
28. Strebhardt K, Ullrich A. Targeting polo-like kinase 1 for cancer therapy. Nat Rev Cancer. 2006;6(4):321–30.
29. Schoffski P. Polo-like kinase (PLK) inhibitors in preclinical and early clinical development in oncology. Oncologist. 2009;14(6):559–70.
30. Owonikoko TK, Zhang G, Deng X, Rossi MR, Switchenko JM, Doho GH, et al. Poly (ADP) ribose polymerase enzyme inhibitor, veliparib, potentiates chemotherapy and radiation in vitro and in vivo in small cell lung cancer. Cancer Med. 2014;3(6):1579–94.
31. Owonikoko TK, Zhang G, Kim HS, Stinson RM, Bechara R, Zhang C, et al. Patient-derived xenografts faithfully replicated clinical outcome in a phase II co-clinical trial of arsenic trioxide in relapsed small cell lung cancer. J Transl Med. 2016;14:111.
32. Liu H, Liu H, Zhou Z, Parise RA, Chu E, Schmitz JC. Herbal formula Huang Qin Ge Gen Tang enhances 5-fluorouracil antitumor activity through modulation of the E2F1/TS pathway. Cell Commun Signal. 2018;16:7.

33. Tsherniak A, Vazquez F, Montgomery PG, Weir BA, Kryukov G, Cowley GS, et al. Defining a Cancer Dependency Map. Cell. 2017;170(3):564–76.e16.
34. Yang W, Soares J, Greninger P, Edelman EJ, Lightfoot H, Forbes S, et al. Genomics of Drug Sensitivity in Cancer (GDSC): A resource for therapeutic biomarker discovery in cancer cells. Nucleic Acids Res. 2013;41(Database issue):D955–D961.
35. Poirier JT, Gardner EE, Connis N, Moreira AL, de Stanchina E, Hann CL, et al. DNA methylation in small cell lung cancer defines distinct disease subtypes and correlates with high expression of EZH2. Oncogene. 2015;34(46):5869–78.
36. Hodgkinson CL, Morrow CJ, Li Y, Metcalf RL, Rothwell DG, Trapani F, et al. Tumorigenicity and genetic profiling of circulating tumor cells in small-cell lung cancer. Nat Med. 2014;20(8):897–903.
37. Valsasina B, Beria I, Alli C, Alzani R, Avanzi N, Ballinari D, et al. NMS-P937, an orally available, specific small-molecule polo-like kinase 1 inhibitor with antitumor activity in solid and hematologic malignancies. Mol Cancer Ther. 2012;11(5):1006–16.
38. Beria I, Bossi RT, Brasca MG, Caruso M, Ceccarelli W, Fachin G, et al. NMS-P937, a 4,5-dihydro-1H-pyrazolo[4,3-h]quinazoline derivative as potent and selective Polo-like kinase 1 inhibitor. Bioorg Med Chem Lett. 2011;21(10):2969–74.
39. Zeidan AM, Ridinger M, Lin TL, Becker PS, Schiller GJ, Patel PA, et al. A Phase Ib Study of Onvansertib, a Novel Oral PLK1 Inhibitor, in Combination Therapy for Patients with Relapsed or Refractory Acute Myeloid Leukemia. Clin Cancer Res. 2020;26(22):6132–40.
40. Horie M, Saito A, Ohshima M, Suzuki HI, Nagase T. YAP and TAZ modulate cell phenotype in a subset of small cell lung cancer. Cancer Sci. 2016;107(12):1755–66.
41. Rudin CM, Poirier JT, Byers LA, Dive C, Dowlati A, George J, et al. Molecular subtypes of small cell lung cancer: A synthesis of human and mouse model data. Nat Rev Cancer. 2019;19(5):289–97.
42. Baine MK, Hsieh MS, Lai WV, Egger JV, Jungbluth AA, Daneshbod Y, et al. SCLC Subtypes Defined by ASCL1, NEUROD1, POU2F3, and YAP1: A Comprehensive Immunohistochemical and Histopathologic Characterization. J Thorac Oncol. 2020;15(12):1823–35.
43. Calbo J, Meuwissen R, van Montfort E, van Tellingen O, Berns A. Genotype-phenotype relationships in a mouse model for human small-cell lung cancer. Cold Spring Harb Symp Quant Biol. 2005;70:225–32.
44. Mollaoglu G, Guthrie MR, Bohm S, Bragelmann J, Can I, Ballieu PM, et al. MYC Drives Progression of Small Cell Lung Cancer to a Variant Neuroendocrine Subtype with Vulnerability to Aurora Kinase Inhibition. Cancer Cell. 2017;31(4):270–85.
45. Vastrik I, D'Eustachio P, Schmidt E, Gopinath G, Croft D, de Bono B, et al. Reactome: A knowledge base of biologic pathways and processes. Genome Biol. 2007;8(3):R39.
46. Yim H, Erikson RL. Plk1-targeted therapies in TP53- or RAS-mutated cancer. Mutat Res Rev Mutat Res. 2014;761:31–9.
47. Liu X, Erikson RL. Polo-like kinase (Plk)1 depletion induces apoptosis in cancer cells. Proc Natl Acad Sci U S A. 2003;100(10):5789–94.
48. Liu X, Lei M, Erikson RL. Normal cells, but not cancer cells, survive severe Plk1 depletion. Mol Cell Biol. 2006;26(6):2093–108.
49. Yim H, Erikson RL. Polo-like kinase 1 depletion induces DNA damage in early S prior to caspase activation. Mol Cell Biol. 2009;29(10):2609–21.
50. Degenhardt Y, Greshock J, Laquerre S, Gilmartin AG, Jing J, Richter M, et al. Sensitivity of cancer cells to Plk1 inhibitor GSK461364A is associated with loss of p53 function and chromosome instability. Mol Cancer Ther. 2010;9(8):2079–89.
51. Sur S, Pagliarini R, Bunz F, Rago C, Diaz LA Jr, Kinzler KW, et al. A panel of isogenic human cancer cells suggests a therapeutic approach for cancers with inactivated p53. Proc Natl Acad Sci U S A. 2009;106(10):3964–9.
52. Lei M, Erikson RL. Plk1 depletion in nontransformed diploid cells activates the DNA-damage checkpoint. Oncogene. 2008;27(28):3935–43.
53. Sanhaji M, Kreis NN, Zimmer B, Berg T, Louwen F, Yuan J. p53 is not directly relevant to the response of Polo-like kinase 1 inhibitors. Cell Cycle. 2012;11(3):543–53.

54. Su Z, Dias-Santagata D, Duke M, Hutchinson K, Lin YL, Borger DR, et al. A platform for rapid detection of multiple oncogenic mutations with relevance to targeted therapy in non-small-cell lung cancer. J Mol Diagn. 2011;13(1):74–84.
55. Liao Y, Yin G, Wang X, Zhong P, Fan X, Huang C. Identification of candidate genes associated with the pathogenesis of small cell lung cancer via integrated bioinformatics analysis. Oncol Lett. 2019;18(4):3723–33.
56. Rausch V, Hansen CG. The Hippo Pathway, YAP/TAZ, and the Plasma Membrane. Trends Cell Biol. 2020;30(1):32–48.
57. Petitjean A, Achatz MI, Borresen-Dale AL, Hainaut P, Olivier M. TP53 mutations in human cancers: Functional selection and impact on cancer prognosis and outcomes. Oncogene. 2007;26(15):2157–65.
58. Olivier M, Hollstein M, Hainaut P. TP53 mutations in human cancers: Origins, consequences, and clinical use. Cold Spring Harb Perspect Biol. 2010;2(1):a001008.
59. Petitjean A, Mathe E, Kato S, Ishioka C, Tavtigian SV, Hainaut P, et al. Impact of mutant p53 functional properties on TP53 mutation patterns and tumor phenotype: Lessons from recent developments in the IARC TP53 database. Hum Mutat. 2007;28(6):622–9.
60. Leroy B, Anderson M, Soussi T. TP53 mutations in human cancer: Database reassessment and prospects for the next decade. Hum Mutat. 2014;35(6):672–88.
61. Meuwissen R, Linn SC, Linnoila RI, Zevenhoven J, Mooi WJ, Berns A. Induction of small cell lung cancer by somatic inactivation of both Trp53 and Rb1 in a conditional mouse model. Cancer Cell. 2003;4(2):181–9.